Excerpt from the Proceedings of the 2011 COMSOL Conference in Stuttgart

Heat and Mass Transfer in a Gypsum Board Subjected to Fire

Benedikt Weber[*,1]
[1] Empa, Swiss Federal Laboratories for Materials Science and Technology
*Überlandstrasse 129, CH-8600 Dübendorf, Switzerland

Abstract: Heat and mass transfer through a gypsum board exposed to fire is simulated and compared to experimental data. The gypsum board is modeled as a porous medium with moist air in the pores. A dehydration front develops at the fire side and travels through the board, consuming energy and releasing water vapor. The vapor migrates through the porous medium by convection and diffusion, and condenses in colder regions away from the fire. The model involves several physics interfaces: Heat Transfer in Porous Media, Darcy's Law, Transport of Concentrated Species, and Weak Form PDE. The main mechanism is heat conduction. Heat convection by vapor transport has little influence, but condensation and evaporation are important for reproducing the experimentally observed temperature plateau.

Keywords: Gypsum, Fire, Heat transfer, Vapor transport, Condensation / evaporation.

1. Introduction

Gypsum boards are commonly used in construction for partition walls. They provide good fire protection capabilities due to dehydration of gypsum at elevated temperatures. Dehydration is an endothermic chemical reaction, which consumes energy and thus acts as a heat barrier.

The effect of dehydration can be introduced in a heat conduction model by a temperature-dependent apparent heat capacity [1, 2]. Such models give good results for engineering purposes but are unable to reproduce some of the details observed in experiments. In particular, they are unable to capture the temperature plateau usually observed in tests at the unexposed face. An obvious extension is to include the vapor produced during dehydration and to consider the corresponding heat convection. Since vapor can condense in colder regions and evaporate again, the heat exchanged by phase change is also important. Several authors have presented models with vapor transport [3–6]. This paper presents the main results of a recent study [7] and gives some details on the COMSOL implementation.

2. Theory

Gypsum consists of an agglomeration of needle-like crystals. It can thus be considered as a porous medium with a relatively high porosity ϕ. The voids are filled with a gaseous mixture of dry air and water vapor and with liquid water.

Ideal gas behavior is assumed and partial pressures are added according to Dalton's law:

$$p_g = p_v + p_a \tag{1}$$

where p_g denotes the total pressure of the gaseous mixture and p_v, p_a are the partial pressures of vapor and air, respectively. Densities are described by

$$\rho_\pi = \frac{p_\pi M_\pi}{RT} \quad \text{for} \quad \pi = a, v, g \tag{2}$$

where M_π is the molar weight and R is the universal gas constant. The temperature is denoted by T.

Gas transport mechanisms are convection and diffusion. The velocity $\mathbf{v}_g$ of the gas mixture is governed by Darcy's law:

$$\mathbf{v}_g = -\frac{\kappa_g}{\mu_g}\nabla p_g \tag{3}$$

where κ_g is the gas permeability and μ_g is the dynamic viscosity. The relative velocity between air and vapor is described by the diffusive mass flux $\mathbf{j}_v$. It is governed by Fick's law:

$$\mathbf{j}_v = -\rho_g D_{eff} \nabla \omega_v \tag{4}$$

where D_{eff} is the effective diffusion coefficient. This coefficient includes the porosity and the tortuosity of the porous medium and has to be determined experimentally. The variable $\omega_v = \rho_v / \rho_g$ is the mass fraction. Saturation is typically very low and liquid water is assumed to be immobile.

Evaporation and condensation of water are governed by the equilibrium between the partial vapor pressure and the vapor saturation pressure. Condensation takes place when the partial vapor pressure exceeds the saturation pressure. Evaporation occurs when the partial vapor pressure is below the saturation pressure and if there is liquid water available. Capillary effects are neglected, since they are not important as indicated by sorption curves [8].

Dehydration is an endothermic chemical reaction, which consumes energy and releases water vapor. The amount of solid material changed into vapor can be determined by thermogravimetric analysis (TGA). For pure gypsum, stoichiometry predicts a loss of 21% of the original mass. In the example considered here, the actual mass loss was only 17% due to nonreacting components in the board. The dehydration enthalpy can be determined experimentally by differential scanning Calorimetry (DSC) or evaluated from thermodynamic tables [9].

3. Governing Equations

The governing equations are those of mass and energy conservation [10]. The fraction of void occupied by liquid water is the saturation S. The volume fraction of the medium occupied by gas is thus $\phi(1-S)$. Taking into the mass sources $\dot{m}_{\text{dehyd}}$ and $\dot{m}_{\text{evap}}$ due to dehydration and evaporation, conservation of gas reads

$$\frac{\partial}{\partial t}\left(\phi(1-S)\rho_g\right)+\nabla\cdot\left(\rho_g\mathbf{v}_g\right)=\dot{m}_{\text{dehyd}}+\dot{m}_{\text{evap}} \quad (5)$$

Conservation of vapor leads to the same equation with the index g replaced by v. Expressing the partial density of vapor by the mass fraction ω_v and substituting Equation (5) yields

$$\phi(1-S)\rho_g\frac{\partial\omega_v}{\partial t}+\rho_g\mathbf{v}_g\cdot\nabla\omega_v+\nabla\cdot\mathbf{j}_v = (1-\omega_v)(\dot{m}_{\text{dehyd}}+\dot{m}_{\text{evap}}) \quad (6)$$

Note the factor $(1-\omega_v)$ in front of the source terms, which appears because mass from other phases is introduced into the gaseous phase. (COMSOL version 4.2 has an extra input for sources from other phases.)

Since liquid water is considered immobile there is no convective term in the conservation equation:

$$\frac{\partial}{\partial t}\left(\phi S\rho_w\right)=-\dot{m}_{\text{evap}} \quad (7)$$

Conservation of energy is expressed as

$$\rho C_p\frac{\partial T}{\partial t}+\nabla\cdot\left(-k_{\text{eff}}\nabla T\right)+\rho_g C_{pg}\mathbf{v}_g\cdot\nabla T = -\left(C_{pa}\mathbf{j}_a+C_{pv}\mathbf{j}_v\right)\cdot\nabla T - \dot{m}_{\text{dehyd}}\Delta H_{\text{dehyd}}-\dot{m}_{\text{evap}}\Delta H_{\text{evap}} \quad (8)$$

where ρC_p and k_{eff} are the volumetric heat capacity and the effective thermal conductivity, respectively, of the porous medium filled with gases and liquid water. The last term on the left-hand side in Equation (8) takes into account the heat transfer due to the moving gaseous mixture, whereas the first term on the right-hand side reflects the energy transport by interdiffusion [11]. Finally, the heat sources are expressed by the mass sources due to dehydration and evaporation times their respective enthalpies of phase change.

4. Boundary conditions

4.1 Thermal boundary conditions

At the cold side, the heat flux is specified including convection and radiation. The inward conductive heat flux is

$$-\mathbf{n}\cdot(-k_{\text{eff}}\nabla T) = h_T(T_{\text{ext}}-T)+\sigma\varepsilon\left(T_{\text{amb}}^4-T^4\right) \quad (9)$$

where h_T is the heat transfer coefficient, σ is the Stefan-Boltzmann constant, and ε is the surface emissivity. The temperatures T_{ext} and T_{amb} both correspond to the room temperature.

At the fire side, a similar boundary condition could be specified. However, in a furnace, the convective temperature and the radiative temperature are not identical. The control temperature specified in the standard relates to the temperature of a plate thermometer which measures a combination of the two contributions. It is thus almost impossible to specify the heat flux imposed by the furnace without additional data. Instead, the measured temperature on the exposed face of the board is specified directly.

4.2 Mass transfer boundary conditions

For the gas mixture, the pressure is specified as the atmospheric pressure on both sides of the board:

$$p_g = p_{\text{atm}} \quad (10)$$

Note that the pressure in the furnace is controlled by ventilation and usually kept close the atmospheric pressure. The vapor transport through the boundary is specified by the vapor flux and is expressed as

$$-\mathbf{n}\cdot(\omega_v\rho_g\mathbf{v}_g+\mathbf{j}_v)=h_v(\rho_v^{\text{amb}}-\rho_v) \quad (11)$$

where h_v is the mass transfer. It is a reduced value accounting for the paper layer covering the gypsum board. The vapor densities are related to the partial vapor pressures. The ambient vapor pressure is determined from the relative humidity.

5. Phase change of water

Condensation and evaporation are implemented by the so-called nonequilibrium formulation. The evaporation mass is calculated as

$$\dot{m}_{\text{evap}} = K \frac{M_w}{RT} \left(p_{\text{sat}} - p_v \right) \qquad (12)$$

This formulation can also be considered as a penalty formulation. The penalty factor K has no direct physical meaning and is chosen on numerical grounds. It has to be large enough to approximately enforce the phase equilibrium but not too large in order to avoid numerical problems like large oscillations.

To avoid evaporation if the saturation is zero, the penalty factor is chosen as

$$K = K_0 \left[1 - H(S_{\min} - S) \cdot H(p_{\text{sat}} - p_v) \right] \qquad (13)$$

where H is the Heaviside function. For the numerical implementation, a smoothed Heaviside (*flc2hs*) function is actually used, which changes smoothly from zero to one in an interval between zero and some small positive value.

6. Material properties

The thermal properties of gypsum are temperature dependent. The effective thermal conductivity of the gypsum board is shown in Figure 1, the bulk density in Figure 2. The time derivative of the bulk density is the dehydrated mass rate $\dot{m}_{dehyd}$. The corresponding heat sink is $\dot{m}_{dehyd} \Delta H_{dehyd}$. Instead if this time-dependent quantity, the apparent heat capacity

$$\left(C_{ps} \right)_{\text{app}} = C_{ps} + \frac{1}{\rho_s} \frac{\partial m_{\text{dehyd}}}{\partial T} \Delta H_{\text{dehyd}} \qquad (14)$$

is shown in Figure 3. It exhibits two peaks corresponding to two reaction steps. Although the temperature of reaction depends on the heating rate and the partial vapor pressure, the peaks are taken at predefined temperatures. All the temperature-dependent properties are defined analytically in terms of smoothed Heaviside functions (*flc2hs*).

The most relevant material parameters for the gypsum board are:

C_{ps}	Heat capacity	1000 J/(kg·K)
ρ_{s0}	Initial mass density	820 kg/m^3
ϕ	Porosity	0.6
$D_{\text{eff}}^{\text{ref}}$	Diffusion coefficient	$8 \cdot 10^{-6}$ m^2/s
κ_g	Gas permeability	$8 \cdot 10^{-14}$ m^2

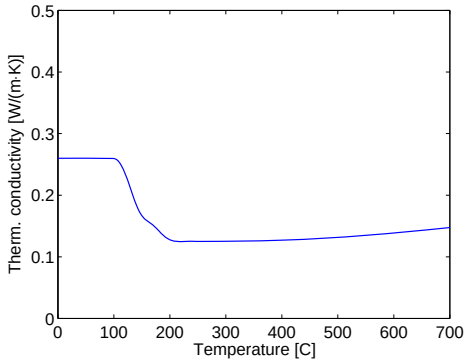

Figure 1: Thermal conductivity of gypsum board

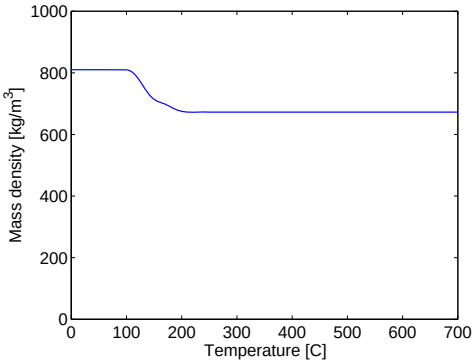

Figure 2: Bulk density of gypsum board

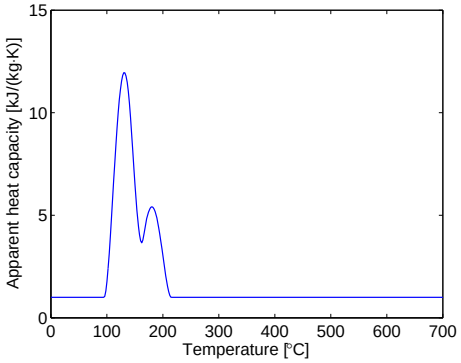

Figure 3: Apparent heat capacity

The effective diffusion coefficient depends on temperature and pressure. Data from [12] is well approximated by

$$D_{\text{eff}} = D_{\text{eff}}^{\text{ref}} \left(\frac{T}{20^\circ\text{C}} \right)^{1.7} \frac{p_{\text{atm}}}{p_g} \qquad (15)$$

COMSOL has built-in material laws for air and water vapor. While air properties are defined up to 1600 K, vapor is only defined up to 850 K. It seemed therefore preferable to define material properties in a user-defined

library. The dynamic viscosity and the heat capacity from room temperature up to 1000°C have been approximated by interpolating values from standard tables [13]. The individual viscosities in Pa·s are

$$\mu_a = 4.9728 \cdot 10^{-6} + 4.8919 \cdot 10^{-8} T - 1.0406 \cdot 10^{-11} T^2$$

$$\mu_v = -2.8334 \cdot 10^{-6} + 4.044 \cdot 10^{-8} T$$

and the viscosity of the mixture is [14].

$$\mu_g = \mu_v + (\mu_a - \mu_v) x_v^{0.608} \qquad (16)$$

where $x_a = p_a / p_g$ is the molar fraction of air.

The individual heat capacities in J/(kg·K) are

$$C_{pa} = 941.46 + 0.19518 \cdot T$$

$$C_{pv} = 2210.4 - 0.81271 \cdot T + 0.00089167 \cdot T^2$$

For the boundary condition, the following coefficients are used:

Exposed face

h_v	Mass transfer coefficient	0.0075 m/s

Unexposed face

h_T	Heat transfer coefficient	8 W/(m^2·K)
h_v	Mass transfer coefficient	0.0015 m/s
ε	Surface emissivity	0.9

The heat transfer coefficient at the unexposed face has been determined from an empirical relationship between the Nusselt number and the Rayleigh number for a horizontal plate heated from below [15]. The mass transfer coefficient has been found by analogy, replacing the Nusselt number by the Sherwood number [15]. For the unexposed face, the mass transfer coefficient has been reduced to account for a paper layer on the gypsum board.

The penalty factor in Equation (13) has been chosen as $K_0 = 50$ 1/s.

7. Use of COMSOL Multiphysics

The models have been developed under version 4.1 and were later run under version 4.2. All simulations have been performed with a one-dimensional model consisting of 20 elements with quadratic shape functions.

Thermodynamic properties and material properties are defined as variables in the Definitions node of the model. Material properties up to 1000°C (viscosity and heat capacity) of water vapor and air are formulated in a user defined library.

The main physics interface is Heat Transfer in Porous Media. In this interface the thermal properties are weighted by the volume fraction of solid and liquid material. However, since the properties are known directly for the porous material, they are all contributed to the solid part ($\theta_p = 1$).

Conservation of gas is directly implemented in the interface Darcy's Law if the porosity is corrected by the saturation. Conservation of vapor is implemented in the interface Transport of Concentrated Species. However, this interface is not designed for porous media and the porosity has to be introduced manually in the weak form equations. Conservation of liquid water has been implemented by a Weak Form PDE.

8. Experimental Results

Experimental data are taken from [2]. In this reference, a 12 mm thick horizontal gypsum board of size 1 m by 0.8 m was heated from below in a furnace with a controlled temperature according to the standard ISO 834-1 curve [16]. Temperatures were recorded at several depths (Figure 4). On the exposed face, the temperature rises up to 700°C in 25 minutes. On the unexposed face, the temperature shows the usual plateau between 5 and 10 minutes. The error bars indicate the variation of measured temperatures at different locations on the board at the same depth. For the discussion, we concentrate on the unexposed face, which is the most interesting and shows the least variations.

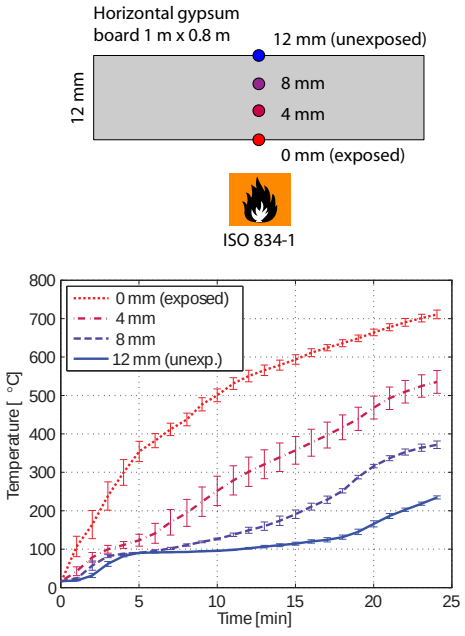

Figure 4: Temperatures measured in experiment

9. Results and Discussion

To show the effect of different mechanisms, simulations are first performed without condensation and evaporation. In a second stage, the effect of phase change is introduced. For comparison, a model with heat conduction only is also used.

9.1 Heat convection by vapor

To explain the results, it is useful to first consider the pressure build-up due to vapor production from dehydration. As shown in Figure 5, the total gas pressure is only little increased from the initial atmospheric pressure (dashed lines). The partial vapor pressure (solid lines) does not reach the total gas pressure, which means that there is always some air present in the mixture. This behavior takes place if the diffusion coefficient is rather high. Reducing its value leads to higher vapor pressures (not shown). Also shown in the figure is the saturation pressure (dotted lines), which is only a function of temperature. Regions where the partial vapor pressure is higher than the saturation pressure indicate potential condensation.

The vapor flux over the thickness in 2-minute intervals is shown in Figure 6. As the dehydration front travels from the fire side (left) to the unexposed side (right), vapor is injected and moves into both directions as seen from the sign of the vapor flux. Positive flux means transport to the unexposed side (right) and negative flux indicates transport to the fire side. The air flux, shown in Figure 7, is almost negligible. Due to the high porosity, the behavior is similar to the free space where injected vapor just spreads out while the air remains more or less still.

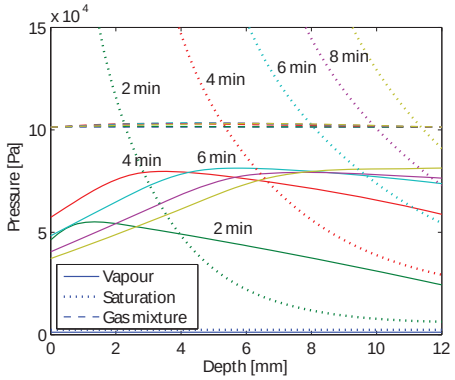

Figure 5: Pressure without condensation

The energy transport by vapor is very low compared to heat conduction, as seen from Figure 8. The temperature at the unexposed face in a model with heat conduction only (conductions) is almost the same as in a model with additional vapor transport (convection). Both curves match the measured curve quite well except for the temperature plateau between 5 and 10 minutes.

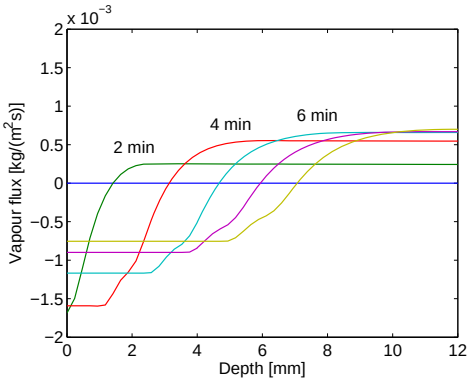

Figure 6: Vapor flux

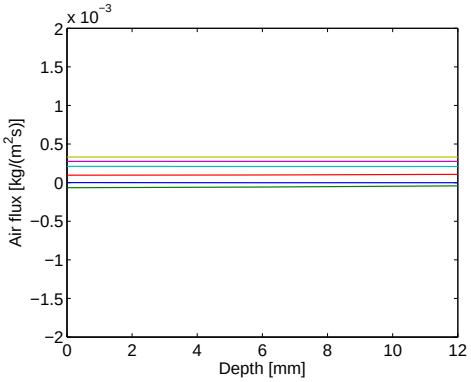

Figure 7: Air flux

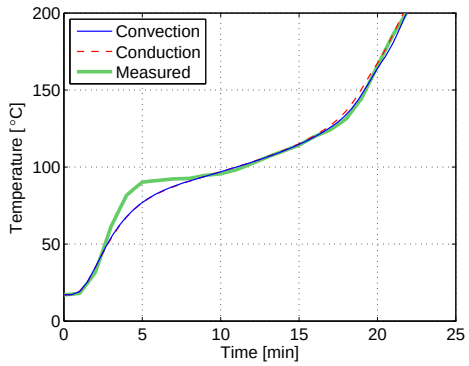

Figure 8: Temperature on unexposed face

9.2 Effect of condensation and evaporation

Vapor produced at the dehydration front moves in both directions as seen from the vapor flux in Figure 6. When it reaches the colder region towards the unexposed face, vapor condenses and later evaporates again. The evolution of the evaporation in 2-minute intervals is shown in Figure 9. Negative values correspond to condensation. The mechanism of condensation and evaporation pushes liquid water to the unexposed face, as shown by the saturation plotted in Figure 10.

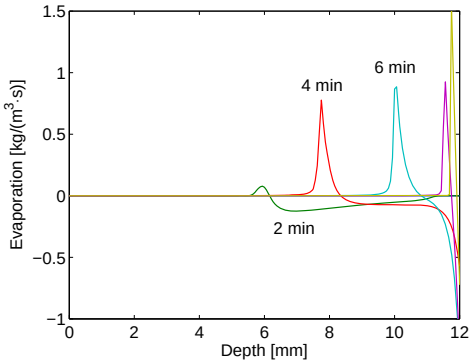

Figure 9: Evaporation

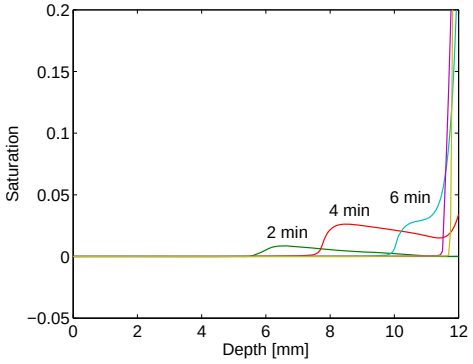

Figure 10: Saturation

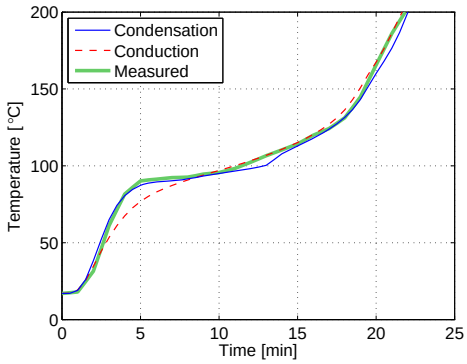

Figure 11: Temperatures on unexposed face

The effect of condensation and evaporation on the temperature is seen in Figure 11. In a first period (up to around 5 minutes), condensation heats up the unexposed face: the slope of the temperature is increased. In a second period (after around 5 minutes), evaporation cools the unexposed face: the slope of the curve is reduced, leading to the plateau. At around 13 minutes, all liquid water has been evaporated and the temperature curve rises again to catch up with the curve of the heat conduction model.

Introducing condensation and evaporation greatly improves the simulated temperature evolution near the plateau. Although there are slight differences in local detail, the general result matches the measurements quite well. It should be kept in mind that the influence of the paper layer has been modeled only approximately by a reduced mass transfer coefficient and that no three-dimensional effects, such as the disturbances by the thermocouple, are considered. Nevertheless the results suggest that the correct mechanisms have been employed in the model.

10. Conclusions

Heat transfer in a gypsum board subjected to fire has been simulated successfully using a model with heat conduction, vapor transport, and condensation and evaporation. The general temperature evolution at the unexposed face is dominated by heat conduction and energy consumption due to dehydration. Heat convection by vapor transport contributes very little and influences the temperature only marginally. However, condensation and evaporation have a significant effect and are responsible for the temperature plateau.

COMSOL is very versatile in modeling different physics. However when coupling many different interfaces, it is advisable to formulate the differential equations and compare them with the equations in the interfaces. Some modifications might be necessary. The high flexibility of COMSOL allowed for evaluating several models of different complexity with little effort.

11. Nomenclature

11.1 Variables

C_p	Heat capacity [J/(kg·K)]
D_{eff}	Effective diffusion coefficient [m^2/s]
H	Enthalpy J/kg
h_T	Heat transfer coefficient [W/(m^2·K)]
h_v	Mass transfer coefficient [m/s]
$\mathbf{j}$	Diffusive mass flux [kg/(m^2·s)]
k_{eff}	Effect. thermal conductivity [W/(m·K)]
$\dot{m}$	Mass source [kg/(m^2·s)]
M	Molar mass [kg/mol]
p	Pressure [Pa]
R	Molar gas constant [J/(mol·K)]
S	Saturation [-]
T	Temperature [K]

11.2 Greek symbols

ΔH	Enthalpy of phase change [J/kg]
ε	Surface emissivity [-]
κ_g	Gas permeability [m^2]
μ	Dynamic viscosity [Pa·s]
ϕ	Porosity [-]
ρ	Mass density (partial) [kg/m^3]
ω	Mass fraction [-]

11.3 Subscripts

a	air
amb	ambient
atm	atmospheric
dehyd	dehydration
evap	evaporation
g	gas mixture
ref	reference
s	solid (gypsum)
std	standard
v	water vapour
w	liquid water

12. References

1. J.R. Mehaffey, P. Cuerrier, and G. Carisse, A model for predicting heat transfer through gypsum-board/wood-stud walls exposed to fire, *Fire and Materials*, **18 (**1994)

2. K. Ghazi Wakili, E. Hugi, L. Wullschleger, and T.H. Frank, Gypsum board in fire – modeling and experimental validation, *Journal of Fire Science*, **25**, 267–282 (2007)

3. S.T. Craft, B. Isgor, G. Hadjisophocleous, and J.R. Mehaffey, Predicting the thermal response of gypsum board subjected to a constant heat flux, *Fire and Materials*, **32**, 333–355 (2008)

4. C.N. Ang, and Y.C. Wang, Effect of moisture transfer on specific heat of gypsum plasterboard at high temperatures, *Construction and Building Materials*, **23**, 675–686 (2009)

5. S.V. Shepel, K. Ghazi Wakili, and E. Hugi, Vapor Convection in gypsum plasterboard exposed to fire: numerical simulation and validation, *Numerical Heat Transfer, Part A: Applications*, **57**, 911–935 (2010)

6. D. Kontogeorgos and M. Founti, Numerical investigation of simultaneous heat and mass transfer mechanisms occurring in a gypsum board exposed to fire conditions, *Applied Thermal Engineering*, **30,** 1461–1469 (2010)

7. B. Weber, Heat transfer mechanisms and models for a gypsum board exposed to fire, under revision in *International Journal of Heat and Mass Transfer* (2011).

8. R.F. Richards, D.M. Burch, and W.C. Thomas, Water vapor sorption measurements of common building materials, *Transactions – American Society of Heating, Refrigerating and Air-Conditioning Engineers*, **98**, 475–475 (1992)

9. K. Kelley, J. Southard, and C. Anderson, Thermodynamic properties of gypsum and its dehydration products, *US Bureau of Mines*, technical paper 625 (1941).

10. S. Whitaker, Conservation equations, in: *Gas Transport in Porous Media*, **20,** 71–120 Springer (2006)

11. E.R.G. Eckert and M. Drake Jr., *Analysis of Heat and Mass Transfer*, MacGraw-Hill (1972)

12. E.A. Mason and L. Monchick, Survey of the equation of state and transport properties of moist gases, in: A. Wexler and W.A. Wildhack (Eds.), *Humidity and Moisture: Fundamentals and Standards*, 257–272, Reinhold Pub. Corp. (1965)

13. VDI-Wärmeatlas, 10th ed., Chapter D, Springer-Verlag, Berlin Heidelberg (2006)

14. D. Gawin, C.E. Majorana, and B.A. Schrefler, Numerical analysis of hygro-thermal behaviour and damage of concrete at high temperature, *Mechanics of Cohesive-Frictional Materials*, **4**, 37–74, (1999)

15. A. Bejan, *Convection Heat Transfer*, Wiley (1984)

16. ISO 834-1, *Fire Resistance Tests – Elements of Building Construction* – Part 1: General Requirements (1999)